Diamond growth in mantle fluids

Hélène Bureau, Daniel J. Frost, Nathalie Bolfan-Casanova, Clémence Leroy, Imène Esteve, Patrick Cordier

Diamond growth in mantle fluids

Hélène Bureau[a*], Daniel J. Frost[b], Nathalie Bolfan-Casanova[c], Clémence Leroy[a], Imène Esteve[a], Patrick Cordier[d]

[a] *Institut de Minéralogie, de Physique des Matériaux et de Cosmochimie (IMPMC), Sorbonne Universités – UPMC Univ. Paris 06, CNRS UMR 7590, Muséum National d'Histoire Naturelle, IRD UR 206, 4 place Jussieu, 75252 Paris Cedex 05, France*

[b] *Bayerisches Geoinstitut, Universität Bayreuth, D-95440 Bayreuth, Germany*

[c] *Laboratoire Magmas et Volcans, Université Blaise Pascal, Clermont-Ferrand, France*

[d] *Unité Matériaux et Transformations, Université Lille 1, 59655 Villeneuve d'Ascq, France*

Revised manuscript for submission to Lithos: SI Diamonds

*Corresponding author.

E-mail address: Helene.bureau@impmc.upmc.fr, Tel. +33 1 44274807

Keywords : diamonds, inclusions, water, chlorine, carbonates

Abstract

In the upper mantle, diamonds can potentially grow from various forms of media (solid, gas, fluid) with a range of compositions (e.g. graphite, C-O-H fluids, silicate or carbonate melts). Inclusions trapped in diamonds are one of the few diagnostic tools that can constrain diamond growth conditions in the Earth's mantle. In this study, inclusion-bearing diamonds have been synthesized to understand the growth conditions of natural diamonds in the upper mantle. Diamonds containing syngenetic inclusions were synthesized in multi-anvil presses employing starting mixtures of carbonates, and silicate compositions in the presence of pure water and saline fluids (H_2O-NaCl). Experiments were performed at conditions compatible with the Earth's geotherm (7 GPa, 1300-1400°C). Results show that within the timescale of the experiments (6 to 30 hours) diamond growth occurs if water and carbonates are present in the fluid phase. Water promotes faster diamond growth (up to 14 mm/year at 1400°C, 7 GPa, 10 g/l NaCl), which is favourable to the inclusion trapping process. At 7 GPa, temperature and fluid composition are the main factors controlling diamond growth. In these experiments, diamonds grew in the presence of two fluids: an aqueous fluid and a hydrous silicate melt. The carbon source for diamond growth must be carbonate (CO_3^2) dissolved in the melt or carbon dioxide species in the aqueous fluid (CO_{2aq}). The presence of NaCl affects the growth kinetics but is not a prerequisite for inclusion-bearing diamond formation. The presence of small discrete or isolated volumes of water-rich fluids is necessary to grow inclusion-bearing peridotitic, eclogitic, fibrous, cloudy and coated diamonds, and may also be involved in the growth of ultradeep, ultrahigh-pressure metamorphic diamonds.

1. Introduction

The growth mechanism of natural diamonds in the Earth's mantle is still an open and debated issue in Earth Sciences (e.g. Stachel and Harris, 2009; Harte, 2010; Shirey et al., 2013 and all references therein). Diamond is a metasomatic mineral that formed through redox reactions of mobile C-bearing phases (fluids/melts) that percolate in the mantle over a large range of depths suggesting different kind of carbon sources. The nature and storage modes for carbon at depth are still poorly understood. This is mostly because, unlike to hydrogen, carbon is not significantly incorporated into the major rock-forming minerals of the mantle but instead forms accessory phases. Depending on the depth these accessory phases may evolve from fluids/melts, carbonates, diamond, Fe-rich alloys, or metal carbide. For that reason diamond growth scenarios in the different mantle regions (upper, transition zone and lower) are still undefined. A systematic investigation of the phases trapped in natural diamonds as inclusions is of primary relevance to constrain diamond genesis as well as to understand carbon storage and cycling in the mantle.

Most natural diamonds are brought up to the Earth's surface through kimberlitic volcanism in ancient cratonic lithosphere, but monocrystalline and sublithospheric diamonds can also be found in alluvial deposits. Due mainly to differences in their inclusions, we distinguish diamonds formed in the lithosphere from those that are formed below the lithosphere in the convecting mantle. The majority of the gem quality monocrystalline diamonds are from the lithosphere. They have eclogitic or peridotitic (the most abundant) associations depending on the mineral assemblage of their inclusions, and come from depths of at least 200 km, based on the phase equilibria of their solid inclusions (Stachel and Harris, 2009; Harte, 2010). Recently, fluid inclusions of high-density saline fluids have been found in very

old monocrystalline diamonds (Weiss et al., 2014) possibly implying a morphological continuum between monocrystalline diamonds and fibrous diamonds, another species of lithospheric diamonds. The later are characterized by their high density of fluid and mineral inclusions (Klein Ben David et al 2010 and references therein). The fluids reflect oxidizing conditions and show a variety of compositions between carbonatitic, silicic and saline end-members. These fluids are the crucial deciphering tools for diamond growth mechanisms as they represent the "medium" in equilibrium during diamond growth (e.g. Navon et al., 1988 Klein BenDavid et al., 2010 and references therein). A final form in which diamonds are found are as polycrystalline assemblages (Heaney et al. 2005) such as framesites (e.g. Kurat and Dobosi, 2000) and carbonados (e.g. Sautter et al., 2011). Carbonados are exclusively found as pebbles within placers and are not known to be associated with kimberlitic rocks, so their origin is still a matter of debate. Moreover carbonados completely lack typical mantle-derived inclusions and may contain assemblages of native minerals and metals (protogenetic inclusions of augite and ilmenite - i.e. seeds for diamond nucleation), pointing to a genesis characterized by highly reducing conditions (FMQ-15 log units, Sautter et al. 2011 and ref. therein). These diamonds are characterized by tiny micrometer-sized crystals found in crustal rocks originally subducted to ultrahigh pressures (e.g. De Corte, et al., 1998; Dobrzhinetskaya, 2012 for a review).

Diamonds grow through metsomatic processes involving C-O-H bearing fluids or melts. The nature of these fluids likely varies depending on the particular diamond forming conditions. It has been proposed, for example, that unlike diamonds from the upper mantle that grow within oxidized fluids, ultra-deep diamonds (i.e. from the lower mantle) derive from reduced fluids (Stachel and Harris, 2009). The recent discovery of a OH-bearing ringwoodite inclusion in a diamond from the transition zone (Pearson et al., 2014) implies that transition zone diamonds may grow from hydrogen-bearing melts or fluids. Diamonds therefore allow carbon behavior

in the deep Earth to be traced but also provide crucial and unique information concerning the deep cycling of other volatile species. Water and halogens, for example, are commonly found as high density fluids (HDF) trapped as inclusions mainly in fibrous, coated and cloudy diamonds (e.g. Navon et al., 1998; Johnson et al., 2000; Izraeli et al., 2001; Burgess et al., 2002; Klein-BenDavid et al., 2007; Tomlinson et al., 2006; 2009; Weiss et al., 2009; Pearson et al., 2014; Weiss et al., 2014). Furthermore, whereas most HDFs are found in fibrous and coated diamonds, a recent report of HDF trapped in monocristalline diamonds from the Phanerozoic carrying a peridotitic signature (Weiss et al., 2014) points to a role of HDF in the growth of these diamond gems.

Indications concerning the parental "fluids" of diamonds and the locus of their growth in the mantle can be obtained by studying the composition of natural inclusions trapped in diamonds (Pearson et al., 2014; Novella et al., 2015), and from the isotopic carbon and nitrogen signatures of diamonds (see the review after Cartigny 2014; Mikhail et al. 2014). The association of diamond growth with subduction zones is frequently proposed because subduction recycles hydrous and relatively oxidized fluids (Stachel et al., 2005). However, this concept is highly debated, based on carbon and nitrogen isotope signatures of natural diamonds (Cartigny et al., 2014). Indeed, most of the natural diamond gems, including fibrous and coated diamonds, exhibit mantle-derived carbon $\delta^{13}C$ ranges from -10 to -5‰ whereas sedimentary carbon, recycled at subduction zones, ranges from -45 to +4‰, with the range for organic matter being -45 to -15‰ and -3 to 4‰ for carbonates (Cartigny et al., 2014). Some diamonds exhibit a light signature with respect to carbon suggesting that the recycled carbon participates to the growth of these diamonds (e.g. Kaminsky and Wirth, 2009, Walter et al., 2011, Mikhail et al. 2013; Thomson et al., 2014; Zedgenizov et al., 2014; Bulanova et al., 2014). This is supported by the oxygen isotope composition of inclusions trapped in superdeep diamonds (Burnham et al., 2015).

An alternative possibility is that the isotopic variability recorded in diamonds might also reflect a fractionation process occurring during diamond formation (e.g. Cartigny et al., 2014). In summary, diamond formation from C-O-H-N-S fluids (or melts) is quite likely but the source and mechanism remain poorly understood (Stachel and Luth, 2015 and references therein).

One way to address these issues is through laboratory experiments. Diamond growth experiments at pressures and temperatures relevant to the Earth's interior have been conducted by numerous researchers over the last decades. Pal'Yanov et al. (1999) were among the first to experimentally demonstrate the practicality of diamond-growth from a mixture of carbonates and water. Since this study, additional experimental studies have shown that diamonds can grow in complex fluid mixtures, including silicates and saline fluids (e.g. Arima et al., 1993; Pal'yanov et al. 2007; Safonov et al., 2007; 2011; Sokol Pal'Yanov, 2008; Pal'Yanov et al., 2007; Pal'Yanov and Sokol, 2009 and references therein; Arima et al., 2010; Fangan and Luth, 2010; Bureau et al., 2012).

Paradoxically, experimental diamond growth has been achieved using numerous fluid mixtures, and this makes the identification of parental fluids of natural diamonds quite difficult. One approach to more tightly constrain the parental fluids of natural diamonds is to reproduce the inclusions found in diamonds during growth experiments. In a previous study Bureau et al. (2012) were successful in growing diamond bearing inclusions from a mixture of silicate, carbonates and water. Depending on experimental conditions (from 7 to 9 GPa, from 1200 to 1700°C), these inclusions comprised aqueous fluids, silicate glasses or minerals. It was shown that water is a key parameter to grow diamond bearing inclusions in the upper mantle, and that diamonds having trapped inclusions must have experienced fast growth rates. The study has showed that depending on the pressure and temperature conditions, upper mantle diamonds are possibly growing from one single supercritical fluid or from two fluids, aqueous fluid and silicate melt, in equilibrium with each other. This preliminary study was performed with simple

149 starting compositions (pure water, iron-free system) and therefore the inclusions trapped in the
150 new experimentally grown diamonds were not representative in composition of the inclusions
151 observed in natural diamonds because, for example, iron was not present in the system.

152 In the present work, we have experimentally grown diamonds from fluids containing
153 significant amounts of water (pure and saline), together with silicates and carbonates (synthetic
154 and natural). Mineralogical assemblages similar to those found as inclusions in natural
155 diamonds are obtained as inclusions in experimentally grown diamonds.

156

157 **2. Materials and methods**

158 Synthetic and natural powders of various compositions were employed as starting materials, as
159 described in Table 1. We have used: (1) the same mixture MELD of synthetic powders already
160 used in a previous study (Bureau et al., 2012), which has the average composition of natural
161 inclusions trapped in fibrous diamonds, from the study of Navon et al. (1998), but is iron-free;
162 (2) SIDB a mixture of MELD mixed with 10 wt.% natural siderite ($FeCO_3$), in order to add
163 iron; and (3) SED, a mixture of 33.33 wt.% of natural pelagic sediment with 66.66 wt.% of a
164 natural Mid Ocean Ridge Basalt (MORB). These powders were loaded into Pt or AuPd capsules
165 together with pure graphite as a carbon source, and either pure water or solutions of H_2O-NaCl
166 (10 and 30 g/l). We used commercial diamond seeds (diameter: 20-30 µm or 40-60 µm)
167 oxidized in a HT furnace at 1000° for 10 minutes in order to modify the surface of the seeds to
168 form cavities that favor inclusion trapping. The capsules were carefully sealed by welding in

169 order to avoid any fluid loss. Each capsule contained 40 wt.% of one of the three powders, 40
170 wt.% of fluid, 10 wt.% graphite, and 10 wt.% diamond seeds.

171 Experiments were performed in multi-anvil devices at BGI, Bayreuth and at LMV, Clermont-
172 Ferrand. The high-pressure assembly comprised a 18 mm edge-length MgO octahedron,
173 together with tungsten carbide anvils of 11 mm edge length truncations. Graphite or $LaCrO_3$
174 heaters were used and temperatures were measured using W(3%Re)–W(25%Re)
175 thermocouples.
176 The experiments were performed at 6-7 GPa and from 1300°C to 1400°C, for run durations
177 between 6 and 30 hours. After each synthesis the experiment was quenched to room temperature
178 before slow decompression. Capsules were weighed before and after opening to check for the
179 presence of aqueous fluids. The remaining solid products were mounted on stubs covered with
180 carbon tape and studied by Scanning Electron Microscopy (SEM) with a Zeiss Crossbeam
181 Neon40 at IMPMC. The interiors of some diamond seeds were exposed using a Focus Ion Beam
182 (FIB). Galium beams were used either with a Zeiss Crossbeam Neon40 at IMPMC (Paris,
183 France) or a FEI Strata DB 235 at IEMN (Lille France). The FIB sections were deposited on
184 silicon wafers for planar investigations. Quantitative chemical analyses were obtained by the
185 energy dispersive X-ray (EDX) technique in conjunction with either an SEM or FIB. The
186 detector was calibrated with a pure copper target at the start of the session to determine the
187 beam current. EDS semi-quantitative analyses were performed and calibrated using
188 international standards employed for electron microprobe analysis in order to perform spectra
189 deconvolution and quantitification. Moreover the quantification was validated using a range of
190 further well characterized standards: a panteleritic galss (KE12, Métrich and Rutherford, 1992),
191 a basaltic glass from Piton de la Fournaise volcano (Bureau et al., 1998), a synthetic albitic
192 glass (EtC, Bureau et al. 2001) and a San Carlos olivine. The resulting precision on the chemical
193 analysis was approximately 1 wt.%.

Transmission Electron Microscopy (TEM) investigations were performed at UMET, Lille (France) using a FEI Tecnai G2-20 twin operating at 200 kV.

3. Results

Details of the experiments are presented in Table 2. Graphite, which was added in excess, remained as large black globules. The solid powdered run products were composed of diamond seeds embedded in a silicate matrix. For all samples we observed glasses either associated with the crystalline matrix (large glassy areas more or less vesiculated, Figure 1B) or embedded within the new diamond grown around the seeds (Figure 1D). The fact that the glass is massive and does not show quench textures is indicative of equilibrium between the two fluids coexisting at high pressure and high temperature: a carbonate-rich silicate melt (quenched as a glass) and an aqueous fluid (lost on opening), and shows that the melt was fluid saturated.

The mineralogical assemblages present in the solid matrix differ depending on the sample set, as described in Table 2.

Set 1 corresponds to samples #H3908, #H3911, #H3912 (Figure 2). Diamond growth on seeds is observed for these 3 samples. The concentration of chlorine in the solution (10 g/l for #H3908, 1400°C, 30 g/l for #H3911 at 1400°C and #H3912 at 1300°C) appears to affect diamond growth. Diamond growth is greater for #H3908 (Figure 2A, 10 g/l NaCl, 6 hours), than for #H3912 (Figure 2C) and #3911 (30 g/l NaCl, 6 and 30 hours respectively). Samples #H3908 and #H3911 are comparable because they were run at the same pressure, temperature and duration conditions but with different salinities. From these two experiments it is possible that the high salinity lowers the rate of diamond growth. Diamonds seeds are covered by small round crystals of carbonates and new octahedral diamonds form on the seed surface in the

preformed inclusion sites (Figure 2D). Samples #H3911 and #H3912, are comparable in pressure and salinity but were performed at 1400°C and 1300°C for 6 and 30 hours respectively. Based on SEM images, we observe less growth on seeds in sample #H3912 than sample #H3911, demonstrating that temperature is one of the main factors controlling diamond growth.

Set 2 corresponds to samples #S5970, #H3913 (Figure 3). In these samples there is a significant increase in the proportion of diamond overgrowth on seeds, a factor of 10 was measured by SEM in the run #S5970 (30 g/l NaCl, 30 hours, figure 3A) compared to the run #H3913 (same conditions, 6 hours, figure 3B). The presence of iron (siderite) affects the mineralogical assemblage of the silicate matrix, which is composed of silicates and carbonates. For sample #S5970 only, we observe small KCl crystals (Figure 3C) probably precipitated from the fluid during the quench. Spontaneously nucleated octahedral diamonds are observed in the solid matrix (Figure 3D).

Set 3 corresponds to sample #H3915 (Figure 1D). This experiment is chlorine free, and diamond growth is observed on all of the seeds. The matrix is composed of olivine, CaMg-carbonates and alumina spinel and vesiculated glass (Figure 1B). This implies that the presence of Cl does not affect the mineralogical assemblage present, when compared to similar experiments performed with pure water.

Set 4 corresponds to samples #209, #210, #211. For this specific series, runs were performed with a natural basalt and a natural pelagic sediment (Ca-carbonate dominant). Diamond growth was observed only in one experiment, sample #210, which was performed at 7 GPa, and 1350°C. For #210 graphite was present, whereas no graphite was added for the run #209. For the experiment #211, performed at lower pressure, 6 GPa, and at 1400°C, a loss of fluid was noticed during the run explaining the absence of diamond growth. In sample #210, spontaneous nucleation of diamond occurred in the matrix (Figure 3). Diamond seeds exhibit trigon features (Figure 4). These etched features might have been formed when the seeds were

heated in the air at 1000°C in a furnace before the run. Trigons may also be due to diamond dissolution in a fluid but this is in contradiction with the presence of new diamond crystals in the matrix (spontaneous growth). We attribute the trigons to a growing process on seeds during the short time scale of the experiment (6 hours). The silicate matrix is composed of MgO-rich glasses, containing Na and Cl (Figure 1C), and Ca-Na carbonates. The experiment in the presence of a fluid phase exhibits very little diamond growth, possibly because very little calcium carbonates is dissolved in the fluid at 1350-1400°C and 6-7 GPa. This would mean that graphite (still present as a globule in the solid product) does not participate in the diamond growth.

Minerals and glasses from experimental sets 1 to 4 have been analyzed by SEM combined with an EDX analyser, as many of the phases are too small to be investigated with an electron microprobe. The analyses all contain a strong carbon signal due to the use of carbon tape for the sample seat and/or due to the presence of the diamond seeds (Table 3). While a glass phase is always present, we observe different mineralogical assemblages depending on the composition of the starting materials. Set 1: minerals present in the matrix are phengite, rutile, Ca,Mg carbonates and coesite. No chlorine is found in the compositions, suggesting that it remained dissolved in aqueous fluids. Set 2: these runs have been performed in the presence of natural siderite, however iron was not detected in the solid phases. In previous experiments it has been shown that siderite can be dissolved in aqueous fluids at high pressure and temperature (Marocchi et al., 2011). Most of the iron may have been either dissolved in the fluid phase, or possibly alloyed with the Pt capsule during the run, as the latter were not Fe-saturated prior to the experiment. Phengite is not observed but olivine, Ca,Mg carbonates, spinel, and small KCl minerals are deposited on the surface of the diamond seeds (that we attribute to precipitation from the fluid at room conditions). Set 3: this experiment performed in the presence of pure water instead of saline fluids exhibits the same mineralogy to that of set

2 (except that KCl precipitates are absent) suggesting that the presence of chlorine does not affect the mineral assemblage. Set 4: experiments have been performed using natural powders of MORB (basalt, Table 1) and pelagic sediments ($CaCO_3$ – SiO_2, Table 1). For this set of experiments the starting materials were crystalline but the final products are mostly glassy suggesting that the conditions of the experiments #209 and #210 were above the solidus.

The presence of chlorine in the system does not affect the mineral assemblages, but it does affect the kinetics of diamond growth. Indeed we observe that when Cl is present in large amounts (30 g/l NaCl, #S3911), we observe less diamond growth than for runs performed with lower concentrations of Cl (10 g/l NaCl, e.g. #H3908). Two experiments were run for durations of 30 hours (#S5970, #H3912), allowing significant diamond growth on seeds despite a high salinity. In experiments performed at 1400-1600°C, 7 GPa, in MgO-SiO_2-H_2O-C-KCl or -NaCl system (water being added as brucite), Fagan and Luth (2010) suggest that NaCl may inhibit diamond growth, whereas KCl favors it. Therefore, a competition would be expected during experiments between water and NaCl, the former favoring growth while the latter inhibits diamond growth. In comparison to Fagan and Luth (2010), our experiments were carried with an excess of fluid water that may have resulted in the overall promotion of diamond growth.

Inclusions are systematically trapped by diamond during diamond growth in experimental sets 1, 2 and 3. The initiation of inclusion formation is observed at the growing surface of diamonds (see Figure 2D). FIB preparation was performed on a selection of diamonds from experimental sets of samples 1 and 2. The diamonds were sliced open on one face and ion beam polished in order to allow trapped inclusions to be observed. Then the diamonds were sliced on the other face in order to obtain 2-5 µm thick sections. The sections are deposited on silicon wafers with the FIB micromanipulator for SEM investigation. The inclusions can be either located along planes, corresponding to the original surface of the oxidized diamond seeds or isolated within the new diamond areas. Inclusions may be (1)

monocrystalline, with different inclusions of different mineralogy appearing close to each other, (2) multi-phased, having trapped different minerals in one cavity together with voids of irregular shape, originally filled with fluid or (3) pure fluid (see Figure 5B). Thus a number of different mineral phases may be associated together, with the same mineralogy as the solid matrix surrounding the diamonds.

In sample #3908 (set 1, Figure 5), inclusions are diamonds, Ca-carbonates, phengites, coesites and rutiles. They have been trapped on a plane, probably corresponding to the original surface of the oxidized diamond seed. The presence of empty non-geometrical isolated cavities in diamonds (voids) shows that aqueous fluid inclusions were trapped as a single fluid at the same time as the mineral phases in the diamonds during their growth (e.g. Figure 5). The presence of a silicate glass in the solid matrix shows that a silicate melt was also present. Therefore the diamonds were growing in the presence of two distinct immiscible fluids, a silicate-carbonate melt (quenched as a glass) and a brine (aqueous salty fluid). We found no evidence for the presence of another fluid phase (molten salt or carbonatitic melt). The compositions of the inclusions obtained using EDX are presented in Table 4. The brines were lost as the inclusions were opened using the gallium beam.

For samples from set 2, the mineral inclusions trapped in the diamonds also exhibit the same mineralogy as the matrix, together with void spaces. The 2µm thick sections obtained from diamonds from sample #S5970 revealed isolated olivine inclusions and Ca-rich carbonate inclusions (Table 4, uncontaminated analysis). A thin section of 90 nm was prepared for TEM investigation with the FIB for sample #S5970 (Figure 6). TEM investigation of the thin section shows evidence for a new growth area limited by grain boundaries, likely remnants of the initial surface of the diamond seeds. This is similar to diamond growth observed in Bureau et al. (2012). For this long duration and high salinity experiment (30 hours, 30 g/l NaCl, 1300°C), the extent of the growth was not as great as for sample #H3908 (6 hours, 10 g/l NaCl, 1400°C),

and corresponds to only a few µm of monocristalline diamond rims, while diamond growth was of more than 10 µm for sample #H3908.

Diamond growth rate is very difficult to measure because the growth is not isomorphic. This implies that to measure the extent of the growth, diamond should be sliced perpendicular to the direction of the growth with the FIB. The limit between the original seeds and the new diamond areas are also difficult to define without transmission microscopy investigation. In the case of the sample #S5970 (Figure 6), which was sliced perpendicularly to a new face, grain boundaries can be observed through investigation with the TEM that show the growth to be of about 2 µm after 30 hours at 1300°C, 7 GPa. This is confirmed by the distance between inclusions and rims observed in other FIB sections performed for the same sample. This corresponds to a maximum rate of 0.07 µm/h (or 584 µm/year).

For sample #H3908 (1400°C, 7 GPa, 6 hours), the growth was the greatest and therefore the fastest. The extent of growth can only be estimated from SEM photographs because the diamond was excavated with FIB parallel to the growth direction in order to expose the inclusions. Approximately 10 µm of growth is estimated, which would correspond to about 1.67 µm/h (or 14 mm/year). This last value is higher than previous rates of crystallization for diamond measured at 0.1–0.3 µm/h in hydrous kimberlite melts (up to 8 wt.% of H_2O) at 7.5 GPa, 1400-1450°C (Palyanov et al., 2015) confirming that excess water favors diamond growth.

To conclude, for the experimental sets 1 and 2 that have been investigated by FIB, the phases present in the matrix (mineral and fluid phases) coexisting with the diamonds are also trapped as multi-phase inclusions within the newly formed diamond. In the case of the experiments performed with starting materials close to natural rock compositions (set 2), the mineralogical assemblages trapped as inclusions are similar to mineralogical assemblages found in natural diamonds from the upper mantle, olivine (major mineral phase of peridotitic

diamonds, e.g. Harte, 2010) and carbonates (e.g. Schrauder and Navon, 1994). For diamonds of set 3, which were not sectioned using FIB, the solid products exhibit the same mineralogy as set 2 (no effect of Cl on the mineralogy but on kinetics) and the same extent of diamond growth, implying that inclusions were trapped during growth. The observations of (1) very poor diamond growth of sample #210 from the set 4 (basalt, calcite and fluid), (2) that calcite was not dissolved in the fluid at these pressure and temperature conditions, and (3) that graphite is still present in the solid products after the experiments: leads us to conclude that diamonds may grow from the carbonates dissolved in the fluid phases and not directly from graphite.

4. Discussion

4.1 Processes for diamond growth in fluids

The diamonds synthetized in this study have grown in two coexisting C-O-H bearing fluids (water or brine + carbonate-rich silicates) at pressures and temperatures relevant to the upper mantle, following a typical mantle geotherm (1400°C, 7 GPa). This is shown by the association of aqueous fluid inclusions and solid silicate inclusions in the synthetic diamonds. Excess water promotes significant diamond growth even at low temperatures (1300°C) and promotes a fast growth process, which is a kinetic prerequisite to the formation of inclusions (Roedder, 1984). Furthemore, the diamonds synthetized during experiments from set 1, 2, and 3 mimic quite closely morphologies observed in natural monocrystalline octahedral and polycrystalline diamonds.

Carbon was present in all experiments as excess graphite and carbonates. The growing medium was buffered by excess water. In experiments from set 1, 2 and 3, graphite and calcium carbonates are still present as solid minerals at the end of the runs (e.g. Ca,Mg-bearing

carbonates Figure 2D), suggesting that only sodium and potassium carbonates have broken-down during the experiments because they were not stable at these pressuresand temperatures or under such fluid saturated conditions. Calcium carbonates would be stable coexisting with fluid/melt at high pressures and temperatures, in agreement with experimental studies performed for dry systems (Shatskiy et al., 2016 and references therein). Alkali carbonates were dissolved in the fluid/melt and have likely participated in diamond growth. Indeed, Pal'Iyanov et al. (1999) have shown that these carbonates are catalyzing diamond growth. Furthermore it has been reported that water-bearing carbonate melts are silicate solvents (Dalton and Presnall, 1998).

Diamonds can be demonstrated to be growing in the presence of these two fluids because (1) they trap fluid and silicate inclusions (Figure 5), (2) the two fluids (aqueous and silicate-carbonate-melt) are not miscible at the conditions of the experiment (Bureau et al., 2012); (3) fluid and glass are present at the quench. We cannot determine whether diamonds are growing from the melt or from the fluid at these pressures and temperatures.

Bureau et al., (2012) suggested the participation of graphite in diamond precipitation. But, the presence of large graphite globules and very little growth observed in experiments performed at conditions where carbonates are not dissolved in the fluid/melt suggests that graphite may not be directly involved in the diamond formation process. Rather diamond formation requires carbon species dissolved in the oxidized fluids/melts. Because aqueous fluids and silicate carbonate-rich melts are both present during the growth (Bureau et al., 2012), an important issue is to determine if diamonds are growing from carbon species in the melt or in the aqueous fluid. At these conditions, in silicate melts carbon must be dissolved as carbonate anions CO_3^{2-} (principally combined with Na, K) or molecular CO_2 (see Holloway and Blank, 1994). Thermodynamic calculations argue that carbon speciation in C-O-H super critical aqueous fluids involves $CO_{2,aq}$ and $CH_{4,aq}$ species with the possible involvement of organic

anions, such as $CH_3CH_2COO^-$, $HCOO^-$, HCO_3^-,, particualry at low temperatures (Sverjensky et al., 2014). Organic C-O-H species have been observed in diamond-bearing ultrahigh-pressure rocks with a subduction origin (Frezzotti et al., 2011). This is also in agreement with *in situ* siderite dissolution experiments in aqueous fluids at the conditions of shallow subduction (i.e. siderite dissolution at 400°C and up to 1.15 GPa, in pure water and saline fluids, Marocchi et al., 2011), where formic acid (HCOOH), and formaldehyde (HCOH) were observed using Raman spectroscopy. At temperatures higher than 850°C and 5 GPa, however, calculations predict that the dominant species would be $CO_{2,aq}$ (similar to silicate melts) and $CH_{4,aq}$ (Sverjensky et al., 2014).

At the experimental conditions investigated in this study, the dominant species in the aqueous supercritical fluids are likely to be H_2O and $CO_{2,aq}$. Two mechanisms are possible: (1) If diamonds are growing from the carbon dissolved in the melt, CO_3^{2-} is involved, and (2) if diamonds are growing from the aqueous fluids, $CO_{2,aq}$ is involved.

Then the following reactions are proposed, involving constituents from both fluids:

Set 1:

$$12\ Al_2O_3 + 4\ MgO + 2\ K_2CO_3 + 16\ SiO_2 + 4\ H_2O_{\text{aq or melt}} + 2\ CO_{2\ \text{aq or melt}}$$

$$=$$

$$4\ K(AlMg)_2(OH)_2(SiAl)_4O_{10\ \text{phengite}} + 4\ C_{\text{Diamond}} + 19\ O_2 \qquad (1)$$

Set 2:

$$3\ Al_2O_3 + 3\ MgO + 2\ (Fe,Mg)CO_3 + 3\ SiO_2 + 2\ K_2CO_3 + 2\ Na_2CO_3 + 3\ CaCO_3$$

$$+ 2\ H_2O_{\text{aq or melt}} + 2\ CO_{2\ \text{aq or melt}}$$

$$=$$

$$(Fe,Mg)_2SiO_{4\ olivine} + MgAl_2O_{4\ spinel} + 10\ C_{Diamond} + 12\ O_2 + (Ca,Mg)CO_3 + 2\ (Na,K)_2(Ca,Mg)Al_2SiO_7H_2O_{\ "Glass"} \quad (2)$$

In both cases diamond formation would result in oxidation of the surrounding medium, in agreement with the idea that diamonds are metasomatic minerals.

The experimental results can be extrapolated to conditions below those of the lithosphere, as the temperature effect was investigated up to 1700°C (Bureau et al., 2012) and shows that the higher the temperature, the more diamonds grow from what is then a single supercritical fluid/melt. Investigation of the effects of pressure was made up to 9 GPa in a previous study (Bureau et al., 2012). In the upper mantle for a fertile peridotite at a temperature of 1200°C, pressure > 6-7 GPa, and relevant fO_2, predicted C-O-H fluid speciation along the upper mantle adiabat suggests that H_2O and CH_4 are the major C-H species in C-O-H fluids (Frost and McCammon, 2008). This is corroborated by Raman characterization of coexisting aqueous fluids and melts at pressures and temperatures relevant to the upper mantle that reveal the presence of CH_3 or CH_4 species, (Mysen and Yamashita, 2010; Mysen, 2013). Diamonds cannot grow from aqueous fluids below the lithosphere. The parent fluid is possibly a water-rich melt (supercritical) that is thermodynamically stable at these depths. It is probably from such a melt that the diamond carrying the recently discovered hydrous ringwoodite inclusion found by Pearson and co-workers (2014) grew.

Another recently discussed aspect concerning diamond growth in fluids is the potential impact of pH drop when diamonds are growing in aqueous fluids at low pressure and temperature conditions (900°C, 5 GPa, Sverjensky and Huang, 2015). Indeed such a drop would enhance diamond precipitation during water-eclogitic rock interactions without changes in oxidation state. In our experiment whatever the speciation of volatiles are, diamond can precipitate. For example, assuming that diamond precipitates from the aqueous fluids, and that

C-O-H species are stable at 7 GPa, 1300-1400°C, a potential reaction may be expressed involving aqueous species (set 1):

$$12\ Al_2O_3 + 8\ MgO + 2\ K_2CO_3 + 16\ SiO_2 + 4\ HCOO^-_{aq} + 8\ H^+_{aq}$$
$$=$$
$$4\ K(Al,Mg)_2(OH)_2(Si,Al)_4O_{10\ phengite} + 6\ C_{Diamond} + 20\ O_2 + 2\ H_2O \quad (3)$$

This equilibrium would be a function of the pH ($-\log[H^+]$) and of the oxygen fugacity (fO_2).

In experiments from sets 1 and 2, the species Na^+_{aq} and Cl^-_{aq} are mutually neutralized (same amounts of HCl and NaOH in the fluid). The pH is determined from the level of interactions between silicates and aqueous fluids. This means that for runs performed at the same pressure, temperature, duration and starting materials, but having15 g/l NaCl or 30 g/l NaCl respectively in the starting solution, the pH should be the same. We observed different diamond growing rates: higher rate of growth for low NaCl content, than for high NaCl content, which cannot be attributed to a pH change.

This does not mean that the pH has no effect on diamond growth, but it means that these experiments are not relevant to constrain a potential pH effect on diamond crystallization in aqueous fluids. In the present study, at constant pH, pressure and temperature the extend of diamond growth is affected by the salinity of the aqueous fluid. It implies that a key parameter for diamond growth is the chemical composition of the fluid and its potential effect on the fO_2.

4.2 Application to natural cases: comparison with upper mantle natural diamonds

About 2 % of natural diamonds gems do contain inclusions (Stachel and Harris, 2008), whether these diamonds are from the upper mantle, the transition zone or the lower mantle (e.g. Shirey et al., 2013 and references therein). Experiments growing inclusion-bearing diamonds are very rare (Bureau et al., 2012). However, comparing inclusions trapped in synthetic diamonds with natural inclusions found in diamond gems is an excellent diagnostic tool to identify the fluids present in the Earth's mantle from which diamonds are growing, and this can be used to describe deep volatiles cycling.

Inclusions trapped in diamonds from experimental sets 1 and 2 are syngenetic with the new diamond rims. They reflect the mineralogical composition of the minerals that crystallize on cooling of the fluid/melts: when phengite, coesite, carbonates and rutile are coexisting with the diamonds, they are also trapped as mineral inclusions in the diamond; when olivine, spinel and carbonates are coexisting with the diamonds, they form the mineralogical assemblage of the inclusions in the diamond. This reproduces inclusion assemblages found in natural diamonds.Inclusions from set 2 are similar to the natural inclusions trapped in diamonds from the upper mantle. Indeed we have found olivine, spinel and $(Ca,Mg)CO_3$ trapped as inclusions, i.e. silicate minerals of upper mantle peridotites whereby carbonates are also accessory phases in the mantle. These minerals are commonly found together with fluids, possibly saline, as inclusions in fibrous diamonds (Navon et al., 1988; Schrauder and Navon, 1994; Izraeli et al. 2001; Klein Ben David et al. 2009). Diamonds from this study are also comparable with monocrystalline diamonds containing inclusions with a peridotite affinity. Saline fluid inclusions have been described in monocrystalline diamonds (Weiss et al., 2014), possibly having a subduction origin (Weiss et al., 2015). Similarities between fibrous and monocrystalline diamonds have already been pointed out based on trace-element signatures (Rege et al., 2010) and from stable isotope geochemistry (Cartigny et al., 2014 and references therein). These results are relevant to the formation of fibrous coated and cloudy diamonds (e.g.

Navon et al., 1988; Schrauder and Navon, 1994; Izraeli et al., 2001; Klein ben David et al., 2007). Because isolated or polycrystalline diamonds spontaneously nucleated in the solid matrix (this study, Bureau et al., 2012), these results are also relevant to diamonds observed as inclusions in minerals from ultrahigh pressure metamorphic rocks of subduction origin that are believed to have grown in subduction zones fluids originating from carbonate dissolution (e.g. Stöckhert et al., 2001; Dobrzhinetskaya, 2012, and references therein; Frezzotti et al., 2014).

A recent study (Jablon and Navon, 2016) based on the comparison of fibrous diamond inclusions with micro-inclusions trapped along twinning surfaces of twinned monocrystalline diamonds proposes that all diamonds were grown from high density fluids (HDFs). They suggest that part or most of lithospheric diamonds were formed by carbonate-bearing fluids, similar to those generate during our experiments. We suggest that when they are trapped in diamonds, inclusions are the key to identify the parent fluids. But the rarity of inclusions in monocrystalline diamonds makes this research difficult. Inclusion bearing diamonds must have experienced fast growth events, which may be successive, with one or more batches of metasomatic fluids, each possibly having different compositions. The growth of fibrous coated and cloudy diamonds, containing high density areas of fluid and solid inclusions should be the result of fast and multiple growth events. This was suggested in 1994 by Boyd and coworkers, based on the study of the carbon and nitrogen isotopic composition of coated diamonds. The dynamic nature of diamond growth may cause zonation between silicate and carbonatitic endmembers observed in kimberlite-related diamonds (e.g. Schrauder and Navon, 1994; Klein-BenDavid et al., 2004; 2007; 2010; Van Rythoven et Schulze 2009; Rege et al. 2010). Zonations are also observed in monocrystalline diamonds (e.g. Araujo et al., 2009; Bulanova et al., 2014). This is also compatible with the observation of multiple dissolution events (Klein-BenDavid et al., 2007).

514 The results from this study do not imply that all inclusions trapped in monocrystalline
515 diamonds must be syngenetic. There is natural evidence for protogenetic inclusions trapped in
516 diamonds either based on isotope geochemistry (e.g. Thomassot et al., 2009) or based on
517 inclusion mineralogy (Agrosi et al., 2016). Pre-existing inclusions can be encapsulated in
518 diamonds during their growth in fluids. Assuming that the rarity of inclusions in
519 monocrystalline diamonds may be due to growth kinetic processes, we suggest that this may be
520 related to the amount of water present in the fluid: the more water present, the greater the
521 efficiency that diamonds trap inclusions. Further experiments are necessary to determine if the
522 presence of water may be a key parameter correlating with the proportion of inclusions trapped
523 in diamonds.

524 We confirm the "fluid/melt" origin of diamonds (e.g. Stachel and Harris, 2009), in showing
525 that it is possible to grow diamonds from a range of different complex fluid compositions,
526 providing they contain both carbonates and water. These inclusions will represent their parental
527 fluid/melt, or are the product of interaction between parental fluid/melt and the surrounding
528 mantle. This is in agreement with natural cases, where depending on the depth of diamond
529 growth, we observe inclusions of: peridotitic or eclogitic mineral assemblages for the
530 lithospheric mantle; intermediate mineral assemblages between basaltic and peridotitic
531 compositions in the transition zone (Kiseeva et al., 2013).

532

533 *4.3 Are subduction zones good diamond factories?*

534

535 It is now recognized that at least some natural diamonds grow from subduction zones fluids,
536 originating from oceanic slabs. Eclogitic diamonds form in the deep mantle lithosphere from
537 trapped eclogitic slabs. Some eclogitic and transition zone diamonds exhibit a negative carbon

isotopic signature corresponding to an organic carbon source (see Cartigny et al., 2014 and Shirey et al., 2013 for reviews). A subduction origin for diamonds from the transition zone is also strongly suggested by the discovery of a hydrous ringwoodite inclusion in a diamond from Juina, Brazil (Pearson et. al., 2014). In this last case fluid releases are thought to be generated by the dehydration melting reactions of wadsleyite, ringwoodite, and dense hydrous Mg-silicates formed in slabs (e.g. Ohtani, 2005). Diamonds containing lower mantle mineralogical assemblages, may also grow in deep subduction environments within that same type of protolith because this is the most likely source of oxidized fluids at these depths (Stachel et al., 2005; Harte, 2010). A few studies argue that ultradeep diamonds are growing from subducted oceanic crust "fluids" (Tappert et al., 2005; Walter et al. 2011, Palot et al. 2014). Schmandt and coworkers (2014) interpret the low seismic velocities below the United States of America to the presence of melt in the lower mantle due to the transformation of ringwoodite in bridgmanite in the subducting slabs. The discovery of saline fluid inclusions in monocrystalline diamonds from the Northwest Territories of Canada are attributed to saline fluids from a subducting slab that would be the source for fluid-rich diamonds (Weiss et al., 2015). Other diamonds from South Africa, however, carrying similar saline inclusions (Weiss et al., 2014) display a mantle-like isotopic signature ($\delta^{13}C$ centered at -5 ‰) incompatible with a carbon origin either from recycled organic matter or recycled carbonates.

Our experiments suggest that subduction zone fluids are probably the best fluids to grow diamonds because they are possibly enriched in both carbon and water. The high variability of isotopic signatures and the variability of inclusion compositions of natural diamonds probably implies that diamonds are growing in the same manner everywhere in the mantle, i.e. from various carbon-rich fluids including fluids recycled from subduction zones.

5. Conclusion

We show that diamonds can grow at upper mantle conditions in mixtures of silicate melts together with aqueous fluid (possibly saline) and carbonates (dissolved in aqueous fluids or in melts). Depending on the location in the mantle, growth will be associated with silicate melts of different compositions. Depending on the depth of the growth (i. e. pressure and temperature), the process will happen in the presence of aqueous fluid and silicate melt or in the presence of a single supercritical fluid/melt. We show that at upper mantle conditions diamonds are growing from oxidized carbon dissolved either in silicate melts (CO_3^{2-}) or in aqueous fluids (CO_{2aq}), but not from graphite. At a constant pH and oxygen fugacity the extent of growth is dependent on the salinity of the aqueous fluid, suggesting that the key parameter for diamond growth is the chemical composition of the fluid. The speciation of volatile species is not critical providing water is present in excess. This process must be fast in order to promote inclusions trapping during growth. We synthesized diamonds with inclusions (minerals and fluids) trapped in syngenesis with the diamonds. These inclusions reflect the composition of the parent fluids. This shows that, when they are preserved, inclusions and their nature are very good diagnostics to constrain diamond growth conditions in the Earth's mantle. This implies that supercritical fluids/melts are present in the upper mantle and possibly at greater depth, where diamonds grow. This also emphasizes the importance of the deep cycling of major (H, C) and minor (halogens) elements in the mantle and their relevance for natural diamond growth processes.

Acknowledgments

The authors thank the staff of the BGI Bayreuth and LMV Clermont for their constant support during the course of this research, with special thanks to Anja Rosenthal, Vera Laurenz and Geeth Manthilake. François Guyot is warmly thanked for his fruitful comments. HB thanks Alisha Clark for a pertinent last reading of the manuscript. We acknowledge Eddy Foy for DRX analyses, Damien Jaujard for providing the MORB sample and Gabriel Carlier for his help in obtaining natural samples. The pelagic sediments were obtained thanks to the Collection of the Museum d'Histoire Naturelle, Cohelper program. The FIB and SEM facility of IMPMC are supported by Région Ile de France Grant SESAME 2006 NOI-07-593/R, INSU-CNRS, INP-CNRS, UPMC, and by the French National Research Agency (ANR) Grant ANR-07-BLAN-0124-01. The FIB facility was also partly supported by the French RENATECH network, and the TEM national facility in Lille (France) was supported by the Conseil Regional du Nord-Pas de Calais, the European Regional Development Fund (ERDF), and the Institut National des Sciences de l'Univers (INSU, CNRS). The national high-pressure facility multi-anvil presses, MLV Clermont-Ferrand, is supported by INSU, CNRS. We acknowledge the Guest Editor S. Shirey for his valuable help and constructive comments during the review process and Sami Mikhail and one anonymous reviewer for their review reports. The present study was supported by Campus France through the PROCOPE Project 26673WC (HB) and the DFG grant 54366326 (DJF), and by the CNRS-INSU, Programme Incitatif Terre Interne, SYSTER 2012 and 2013 to HB.

Bibliography

609 Agrosi G., Nestola, F., Tempesta, G., Bruno, M., Scandale, E., Harris, J., 2016. X-ray
610 topographic study of a diamond from Udachnaya : Implications for the genetic nature of
611 inclusions. Lithos, 248-251, 153-159.
612
613 Araujo, D.P., Griffin, W.L., O'Reilly, S.Y., 2009. Mantle melts, metasomatism and diamond
614 formation: Insights from melt inclusions in xenoliths from Diavik, Slave craton. Lithos, 112S,
615 675-682.

616 Arima, M., Nakayama, K., Akaishi, M., Yamaoka, S., Kanda, H., 1993. Crystallization of
617 diamond from a silicate melt of kimberlite composition in high-pressure and high-temperature
618 experiments. Geology, 21, 968-970.

619 Arima, M., Kozai, Y., Akaishi, M., 2010. Diamond nucleation and growth by reduction of
620 carbonate melts under high-pressure and high-temperature conditions. Geology, 30, 8, 691-694.

621 Boyd, S.R., Pineau, F., Javoy, M., 1994. Modelling the growth of natural diamonds, Chem.
622 Geol 116, 29-42.

623 Bulanova, G.P., Wiggers de Vries, D.F., Pearson, D.G., Beard, A., Mikhail, S., Smelov, A.P.,
624 Davies, G.R., 2014. An eclogitic diamond from Mir pipe (Yakutia), recording two growth
625 events from different isotopic sources. Chemical Geology, 381, 40-54.

626 Bureau, H., Pineau, F., Métrich, N., Semet, M., Javoy, M. (1998). A melt and fluid inclusion
627 study of the gas phase at Piton de la Fournaise volcano (Réunion Island) – Chem. Geol., 147,
628 115-130.

629 Bureau, H., Keppler, H., Métrich, N. (2000) Volcanic degassing of bromine and iodine :
630 experimental fluid/melt partitioning data and applications to stratospheric chemistry, Earth and
631 Planet. Sci. Let., 183, 51-60.

632 Burgess, R., Layzelle E., Turner G., Harris, J.W., 2002. Constrains on the age and halogen
633 composition of mantle fluids in Siberian coated diamonds. Earth and Planet., Sci., Let., 197,
634 193-203.

635 Bureau, H., Langenhorst, F., Auzende, A.-L., Frost, D.J., Estève, I., Siebert, J., 2012. The
636 growth of fibrous, cloudy and polycrystalline diamonds, Geochimica et Cosmochimica Acta,
637 77, 202-214.

638 Cartigny, P., Palot, M., Thomassot, E., Harris, J.W., 2014. Diamond formation: A stable isotope
639 perspective. Annual reviews in Earth and Planetary sciences, 42, 699-732.
640

641 Dalton, J.A., Presnall, D.C., 1998). The continuum of primary carbonatitic-kimberlitic melt
642 compositions in equilibrium with lherzolite: data from the system CaO-MgO-Al_2O_3-SiO_2-CO_2
643 at 6 GPa. J. Petrol. 39, 1953-1964.
644

645 De Corte, K., Taylor, W.R., De Paepe, P., 2002. Inclusion contents of microdiamonds from
646 UHP metamorphic rocks of the Kokchetav massif, in: C.D. Parkinson, I. Katayma, J.G. Liou,
647 S. Maryama (Eds.), The Diamond-Bearing Kokchetav Massif, Universal Academy Press, Inc.,
648 Kazakhstan, pp. 115–135.
649

650 Dobrzhinetskaya, L.F., 2012. Microdiamonds – Frontier of ultrahigh-pressure metamorphism:
651 A review. Gondwana research 21, 207-223.
652

653 Fagan, A.J., Luth, R.W., 2010. Growth of diamond in hydrous silicate melts. *Contrib. Mineral.*
654 *Petrol*., doi 10.1007/s00410-010-0528-9.

655 Frezzotti, M.L., Huizenga, J.M., Compagnoni, R., Selverstone, J., 2014. Diamond formation by
656 carbon saturation in C-H-O fluids during cold subduction of oceanic lithosphere. Geochimica
657 et Cosmochimica Acta, 143, 68-86.

658 Frost, D.J., McCammon, C.A., 2008. The redox state of Earth's mantle, Annu. Rev. Earth
659 Planet. Sci. 36, 389-420.

660 Haggerty, S.E. 1999. A diamond trilogy: superplumes, supercontinents and supernovae Science
661 285, 851-860.

662 Harte, B., 2010. Diamond formation in the deep mantle: the record of mineral inclusions and
663 their distribution in relation to mantle dehydration zones. Mineralogical Magazine, 74(2), 189-
664 215.

665 Holloway, J.R., Blank, J.G., 1994. Application of experimental results to C-O-H species in
666 natural melts, in Volatiles in Magmas, Rev. in Mineralogy, 30, 187-230.

667 Izraeli, E.S., Harris, J.W., Navon, O., 2001. Brine inclusions in diamonds: a new upper mantle
668 fluid, Earth and Planet., Sci., Let., 187, 323-332.

669 Jablon, B.M., Navon, O. (2016) Most diamonds were created equal. Earth and Planet. Sci. Let.
670 443, 41-47.

671 Johnson, L.H., Burgess, R., Turner, G., Milledge, H.J., Harris, J.W., 2000. Noble gas and
672 halogen geochemistry of mantle fluids: comparison of African and Canadian diamonds.
673 Geochimica et Cosmochimica Acta 64, 717-732.

674 Kiseeva, E. S., Yaxley, G. M., Stepanov, A. S., Tkalcić, H., Litasov, K. D., Kamenetsky, V. S.
675 (2013). Metapyroxenite in the mantle transition zone revealed from majorite inclusions in
676 diamonds. Geology, 41, 883-886.

677 Klein BenDavid, O., Izraeli, E.S., Hauri, E., Navon, O., 2004. Mantle fluid evolution – a tale
678 of one diamond. Lithos, **77**, 243-253.

679 Klein BenDavid, O., Izraeli, E.S., Hauri, E., Navon, O., 2007. Fluid inclusions in diamonds
680 from the Diavik mine, Canada and the evolution of diamond-forming fluids. Geochimica et
681 Cosmochimica Acta 71, 723-744.

682 Klein BenDavid, O., Lovinova, A.M., Schrauder, M., Spetius, Z.V., Weiss, Y., Hauri, E.H.,
683 Kaminsky, F.V., Sobolev, N., Navon, O., 2009. High-Mg carbonatitic microinclusions in some
684 Yakutian diamonds – a new type of diamond-forming fluids. *Lithos*, 112S, 648-659.

685 Klein BenDavid, O., Pearson, D.G., Nowell, G.M., Ottley, C., McNeill, J. C.R., Cartigny, P.,
686 2010. Mixed fluid sources involved in diamond growth constrained by Sr-Nd-Pb-C-N- isotopes
687 and trace elements. Earth and Planet. Sci. Let. 289, 123-133.

688 Kurat, G., Dobosi, G., 2000. Garnet and diopside-bearing diamondites (Framesites),
689 Mineralogy and Petrology 69, 143-159.

690 Marocchi, M., Bureau, H., Fiquet, G., Guyot, F., 2011. In-situ monitoring of the formation of
691 carbon compounds during the dissolution of iron (II) carbonate (siderite). Chem. Geol. 290,
692 145-155.

693

694 Metrich, N., Rutherford, M.J. (1992) Experimental study of chlorine behavior in hydrous silicic
695 melts. Geochimica et Cosmochimica Acta 56, 607-616.

696

697

698 Mikhail, S.,Dobosi, G., Verchovsky, A.B., Kurat, G., Jones, A.P. (2013) Peridotitic and
699 websteritic diamondites provide new information regarding mantle melting and metasomatism
700 induced through the subduction of crustal volatiles. Geochim. et Cosmochim. Acta, 107, 1-11.

Mikhail, S., Verchovsky, A.B., Howell, D., Hutchinson, M.T., Southworth, R., Thomson, A.R., P., Warburton, Jones, A.P., Milledge, H.J., 2014. Constraining the internal variability of the stable isotopes of carbon and nitrogen within mantle diamonds. Chemical Geology 366, 14-23.

Mysen, B.O., Yamashita, S., 2010. Speciation of reduced C-O-H volatiles in coexisting fluids and silicate melts determined in situ to 1.4 GPa and 800°C. Geochimica et Cosmochimica Acta 74, 4577-4588.

Mysen, B.O., 2013. Structure-property relationships of COHN-saturated silicate melt coexisting with COHN fluid: a review of in situ, high temperature, high-pressure experiments. Chemical Geology 346, 113-124.

Navon, O., Hutcheon, I.D., Rossman, G.R., Wasserburg, G.J., 1988. Mantle-derived fluids in diamond micro-inclusions. Nature 335, 784-789.

Novella, D., Bolfan-Casanova, N., Nestola, F., Harris, J.W., 2015. H_2O in olivine and garnet inclusions still trapped in diamonds from the Siberian carton: Implications for the water content of cratonic lithosphere peridotites. Lithos 230, 180-183.

Ohtani, E., 2005. Water in the mantle, Elements, 1, 25-30.

Palot, M., Cartigny, P., Viljoen, F., 2009. Diamond origin and genesis: A c and N stable isotope study on diamonds from a single eclogitic xenolith (Kaalvallei, South Africa). Lithos 112S, 758-766.

725 Pal'yanov, Y.N., Sokol, A.G., Bozdov, Y.M., Khokhryakov, A.F., Sobolev, N.V., 1999.
726 Diamond formation from mantle carbonate fluids, Nature, 400, 417-418.

727 Pal'Yanov, Y.N., Sokol, A.G., Bozdov, Y.M., Tomilenko, A.A., Khokhryakov, Z.F., Sobolev,
728 N.V., 2002. Diamond formation through carbonate-silicate interaction. *Amer. Mineral.*, **87**,
729 1009-1013.

730 Pal'Yanov, Y.N., Sokol, A.G., Tomilenko, A.A., Sobolev, N.V., 2005. Conditions of diamond
731 formation through carbonate-silicate interaction. Eur. J. of Mineral. 17, 207-214.

732 Pal'Yanov, Y.N., Shatsy, V.S., Soblev N., Sokol A.G. (2007) The role of mantle ultrapotassic
733 fluids in diamond formation, Proceedings of the National Academy of Sciences, 104, 9122-
734 9127.

735 Pal'Yanov, Y.N., Sokol, A.G., 2009. The effect of composition of mantle/fluid melts on
736 diamond formation processes. Lithos 112S, 690-700.

737 Pal'Yanov, Y.N., Sokol, A.G., Khokhryakov, A.F., Kruk, A.N., 2015. Conditions of diamond
738 crystallization in kimberlite melt: experimental data. Russian Geology and Geophysics 56, 196-
739 210.

740 Pearson, G., Brenker, F.E., Nestola, F., McNeill, J., Nasdal, L., Hutchison, M.T., Matveev, S.,
741 Mather, K., Silversmit, G., Schmitz, S., Vekemans, B., Vincze, L., 2014. Hydrous mantle
742 transition zone indicated by ringwoodite included within diamond. Nature, 507, 221-224.

743

744 Rege, S., Griffin, W.L., Pearson, N.J., Araujo, D., Zedgenizov, D., O'Reilly, S.Y., 2010. Trace-
745 element pattern of fibrous and monocrystalline diamonds: Insights into mantle fluids. *Lithos*,
746 118, 313-337.

747

748 Roedder, E., 1984. Fluid inclusions, Reviews in Mineralogy 12.

Safonov, O.G., Perchuk, L.L., Litvin, Y.A., 2007. Melting relations in the chloride-carbonate-silicate systems at high-pressure and the model for formation of alkali diamond-forming liquids in the upper mantle. Earth and planet. Sci. Let. 253, 112-128.

Sautter, V., Lorand, J.P., Cordier, P., Bondeau, B., Leroux, H., Ferraris, C., Pont, S., 2011. Petrogenesis of mineral micro-inclusions in an uncommon carbonado. Eur. J. Mineral. 23, 721-729.

Schrauder, M. and Navon, O. 1994. Hydrous and carbonatitic mantle fluids in fibrous diamonds from Jwaneng, Bostwana, Geochim. et Cosmochim. Acta, 58, 761-777.

Shirey, S.B., Cartigny, P., Frost, D.J., Keshav, S., Nestola, F., Nimis, P., Pearson, G., Sobolev, N., Walter, M.J., 2013. Diamonds and the geology of mantle carbon, in Reviews in Mineralogy, 75, 355-421.

Shatskiy, A., Litasov, K.D., Palyanov, Y.N., Ohtani, E. (2016) Phase relations on the K_2CO_3-$CaCO_3$-$MgCO_3$ join at 6 GPa and 900-1400°C: Implications for incipient melting in carbonated mantle domains. Amer. Mine. 101, 437-447.

Schmandt, B., S. D., Jacobsen, T. W., Becker, Z. X., Liu, K. G,. Dueker, 2014. Dehydration melting at the top of the lower mantle. Science, 344, 1265-1268.

Schrauder, M., Navon, O., 1994. Hydrous and carbonatitic mantle fluids in fibrous diamonds from Jwaneng, Bostwana, Geochimica et Cosmochimica Acta 58, 761-771.

774 Sokol, A.G., Tomilenko, A.A., Pal'Yanov, Y.N., Bozdov, Y.M., Pal'Yanova, G.A.,
775 Khokhryakov, A.F., 2000. Fluid regime of diamond crystallization in carbonate-carbon
776 systems. Eur. J. of Mineral. 12, 367-375.

777 Sokol, A.G., Pal'Yanov, Y.N., 2008. Diamond formation in the system MgO-SiO_2-H_2O-C at
778 7.5 GPa and 1600°C. Contrib. Mineral. Petrol., 155, 33-43.

779 Stachel, T., Brey G.P., Harris, J.W., 2005. Inclusions in sublithospheric diamonds: glimpses of
780 the deep Earth. Elements, 1, 73-78.

781 Stachel, T., Harris, J.W., 2008. The origin of cratonic diamonds – Constraints from mineral
782 inclusions. Ore Geology reviews, 34, 4-32.

783 Stachel, T, Harris, J.W., 2009. Formation of diamonds in the Earth's mantle, J. Phys. Condens.
784 Matter, 21, 364206.
785

786 Stachel, T., Luth, R.W. (2015) Diamond formation – Where, wen and how ? Lithos, 220-223,
787 200-220.
788

789 Stöckhert, B., Duyster, J., Trepmann, C., Massonne, C., 2001. Microdiamond daughter crystals
790 precipitated from supercritical COH + silicate fluids included in garnet, Erzebirge, Germany.
791 Geology, 29, 391-394.
792

793 Sverjensky, D.A., Stagno, V., Huang, F., 2014. Important role for organic carbon in subduction-
794 zone fluids in the deep carbon cycle. Nature Geosciences, DOI:10.1028/NGEO2291.
795

796 Sverjensky, D.A., Huang, F., 2015. Diamond formation due to a pH drop during fluid-rock
797 interactions. Nature Communications, DOI: 10.1038/ncomms9702.

798

799 Tappert, R., Stachel, T., Harris, J.W., Muehlenbachs, K., Ludwig, T., Brey, G.P., 2005.
800 Subducting oceanic crust: the source of deep diamonds. Geology 33 (7), 565-568.

801

802 Thomassot, E., Cartigny, P., Harris, J.W., Lorand, J.P., Rollion-Bard, C., Chaussidon, M.
803 (2009). Metasomatic diamond growth: A multi-isotope study (^{13}C, ^{15}N, ^{33}S, ^{34}S) of sulphide
804 inclusions and their host diamonds from Jwaneng (Botswana). Earth and Planet. Sci. Let., 282,
805 79-90.

806

807 Thomson, A.R., Kohn, S.C., Bulanova, G.P., Smith, C.B., Araujo, D., EIMF, Walter, M.J.
808 (2014) Origin of sub-lithospheric diamonds from the Juina-5 kimberlite (Brazil): constraints
809 from carbon isotopes and inclusion. Contrib. Mineral. Petrol. 168: 1081.

810

811 Tomlinson, E.L., Jones, A.P., Harris, J.W., 2006. Co-existing fluid and silicate inclusions in
812 mantle diamond, Earth and Planet., Sci., Let., 250, 581-595.

813

814 Tomlinson, E.L., Müller, W., EIMF, 2009. A snapshot of mantle metasomatism: Trace element
815 analysis of coexisting fluid (LA-ICP-MS) and silicate (SIMS) inclusions in fibrous diamonds.
816 Earth and Planet., Sci., Let., 279, 362-372.

817 Van Rythoven, A.D., Schulze, D.J., 2009. In-situ analysis of diamonds and their inclusions
818 from the Diavik Mine, Northwest Territorries, Canada: Mapping diamond growth. Lithos 112S,
819 870-879.

820 Walter, M.J., Kohn, S.C., Araujo, D., Bulanova, G.P., Smith, C.B., Gaillou, E., Wang, J., Steele,
821 A., Shirey, S.B. (2011) Deep mantle cycling of oceanic crust: Evidence from diamonds and
822 their mineral inclusions. Science, 334, 6052, 54-57.

823 Weiss, Y., Kessel, R., Griffin, W.L., Kiflawi, I., Klein BenDavid, O., Bell D.R., Harris, J.W.,
824 Navon, O., 2009. A new model for the evolution of diamond-forming fluids: Evidence from
825 microinclusion-bearing diamonds from Kankan, Guinea, Lithos, 112S, 660-674.

826

827 Weiss, Y., Kiflawi, I., Davies, N., Navon, O., 2014. High-density fluids and the growth of
828 monocrystalline diamonds. Geochimica et Cosmochimica Acta 141, 145-159.

829

830 Weiss, Y., McNeill, J., Pearson, G., Nowell, G.M., Ottley, C.J., 2015. Highly saline fluids from
831 a subducting slab as the source for fluid-rich diamonds. Nature 524, 339-344.

832

833 Zedgenizov, D.A., Kagi, H., Shatsky, V.S., Razogin, A.L. (2014. Local variations of carbon
834 isotope composition in diamonds from Sao-Luis (Brazil): Evidence for heterogeneous carbon
835 reservoir in sublithospheric mantle. Chem. Geol. 363, 114-124.

836

837

838 **Figure captions**

839

840 **Fig.1:** SEM pictures of A. starting diamond seeds; B. Vesiculated glass (exp #H3915), shows
841 that the fluid phase was present during the whole run. Vesicles are created by water exsolution
842 from the high pressure fluid/melt during the experimental quench (i.e. decompression); C. Glass
843 (exp #210); D. Grown seeds covered by a thin glassy film (exp #H3915).

844 **Fig. 2:** SEM pictures of the solid products from the set of experiments 1: A. exp #H3908,
845 diamond growth on seeds; B. exp #H3911 diamond growth on seeds; C. exp #3912, diamond
846 growth on seeds, in this last case the growth is smaller than for the two previous runs; D. surface
847 of a diamond from exp #H3908. One can observe small new diamonds and carbonate crystals
848 being trapped as inclusions in the growing surface of the diamond seed.

849 **Fig. 3:** SEM pictures of the solid products from the set of experiments 2: A. growth on diamond
850 seeds from exp #S5970, after a long run of 30 hours duration. The growth is spectacular
851 compared to short run times. Trapping of inclusions occurs at the surface of the growing
852 diamond; B. growth on diamond seeds, exp #H3913 (short run: 6 hours); C. small cubic crystals
853 of KCl at the surface of diamond seeds (#S5970); D. spontaneous nucleation of diamond
854 crystals in the matrix, run #S5970.

855

856 **Fig. 4:** SEM pictures of the solid products from the set 4, experiment #210: A. spontaneous
857 nucleation and growth of diamond in the matrix; B. trigons observed at the surface of the
858 diamond seeds attributed to growth on seeds.

859 **Fig. 5:** SEM pictures of one diamond seed from run #H3908. A. The diamond has been opened
860 with FIB and exhibits primary multi-phased inclusions trapped during diamond growth. B. A
861 zoom of the inclusion area together with EDX analysis (see Table 4) shows that these inclusions

862 are of different compositions: Ca-carbonates, coesite, phengite, rutile and diamonds in grey.
863 Empty cavities that lack a geometric shape do likely correspond to lost fluid inclusions. C. SEM
864 picture of the left area, showing small new diamonds, carbonates, coesite and open cavities (i.e.
865 lost fluid); D. SEM picture of the right area, showing phengite, rutile, and open fluid inclusions.

866 **Fig. 6:** Sample #S5970 (7 GPa, 1300°C, 30 hrs). A. Scanning electron microscopy micrograph
867 of one diamond seed having experienced diamond growth before preparation. The double line
868 represents the thin section position that was sliced by focused ion beam B. Thin section of about
869 200 nm thickness for transmission electron microscopy (TEM) study. C. TEM bright field
870 micrograph reconstruction of part of the thin section. This bright field image exhibits several
871 dark contours (wavy lines) originating from diffraction contrast. One can observe new growth
872 areas at the peak of the thin section delimited by grain boundaries. Grain boundaries are also
873 observed within the seed, corresponding to healed fractures as the synthetic diamond seeds have
874 been crushed and pre-oxidized in the air before the experiments. D. Enlargement of the TEM
875 bright field photograph of the peak of the thin section where one can see the grain boundaries
876 corresponding to remnants of the surface of the starting diamond seed. E. High resolution
877 micrograph of one growth area. TEM investigation shows that the new diamond areas are
878 undistinguishable from the initial diamond from a crystallographic point of view (i.e. same
879 crystal orientation).

880

881

882

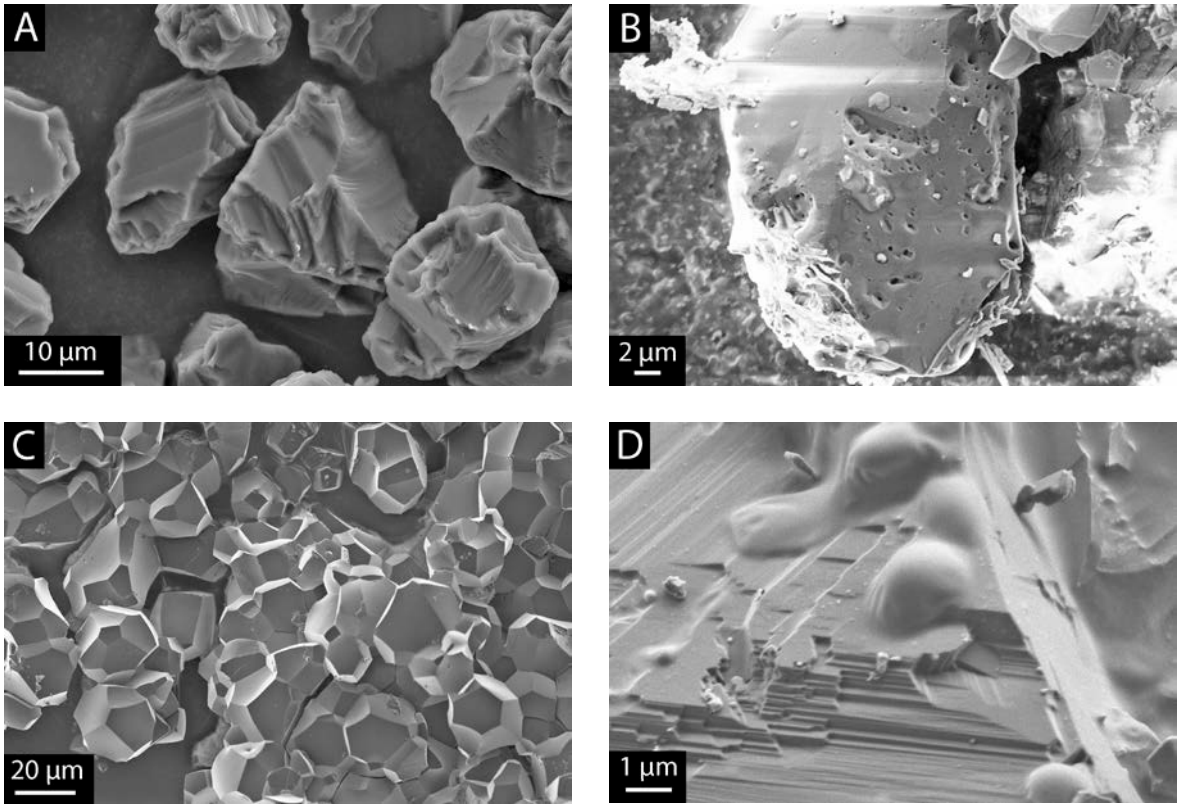

Figure 1

883
884

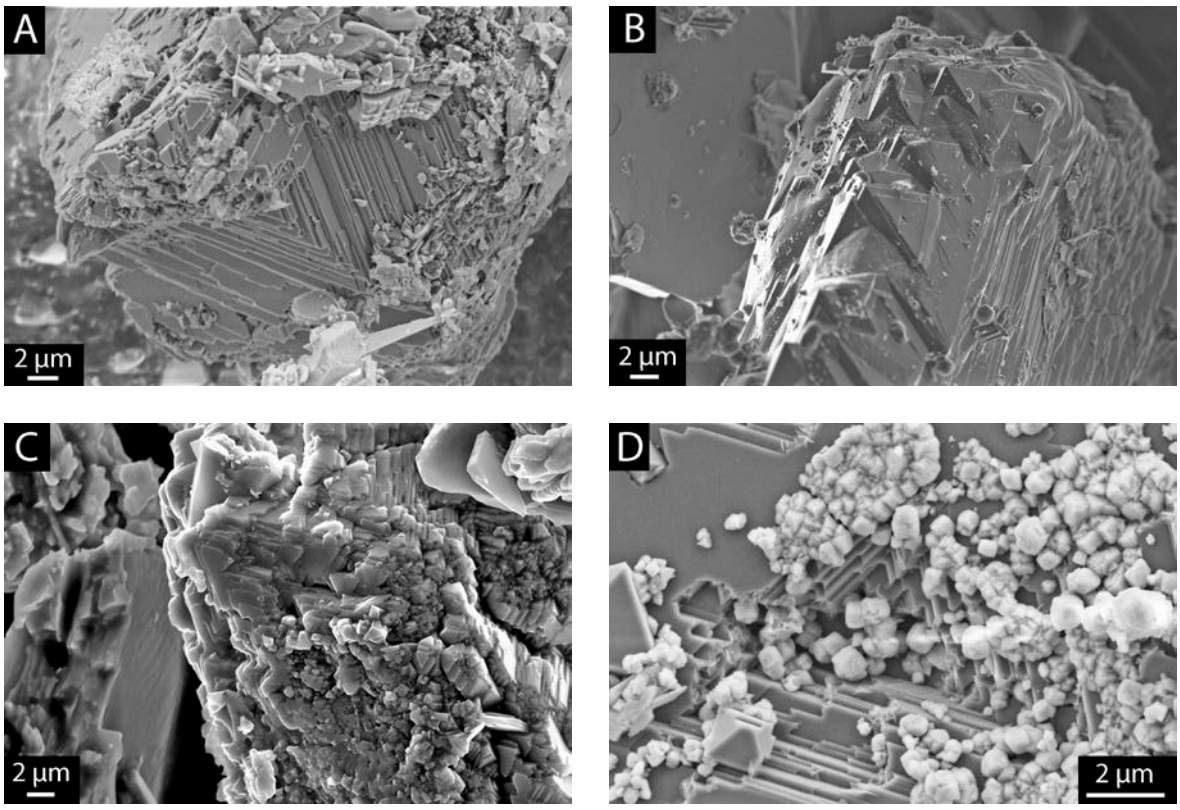

Figure 2

885

886

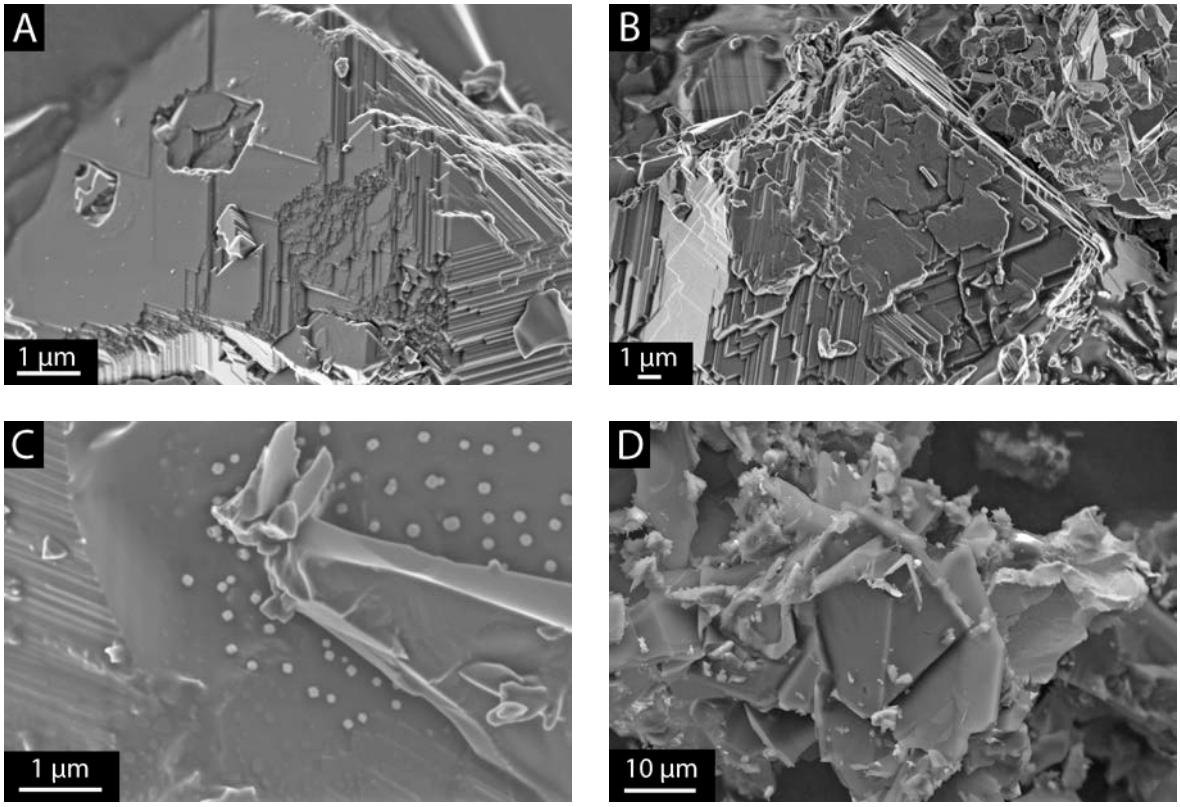

Figure 3

887

888
889

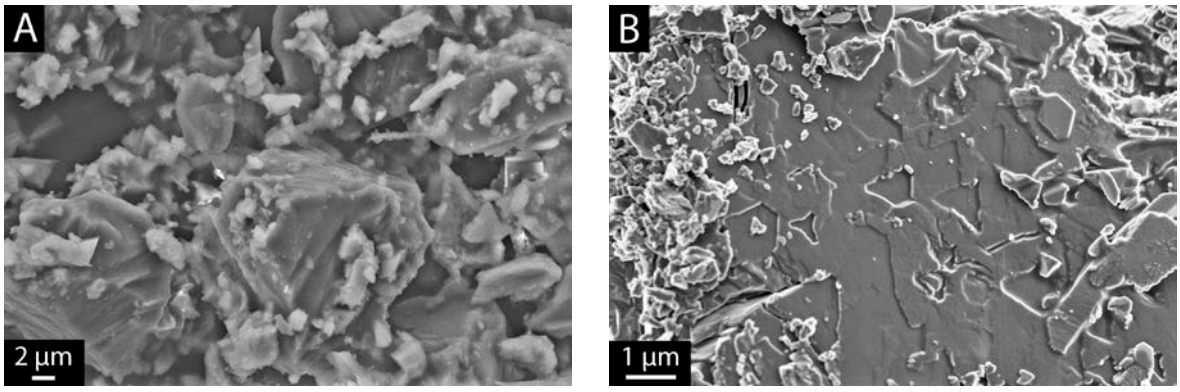

Figure 4

890

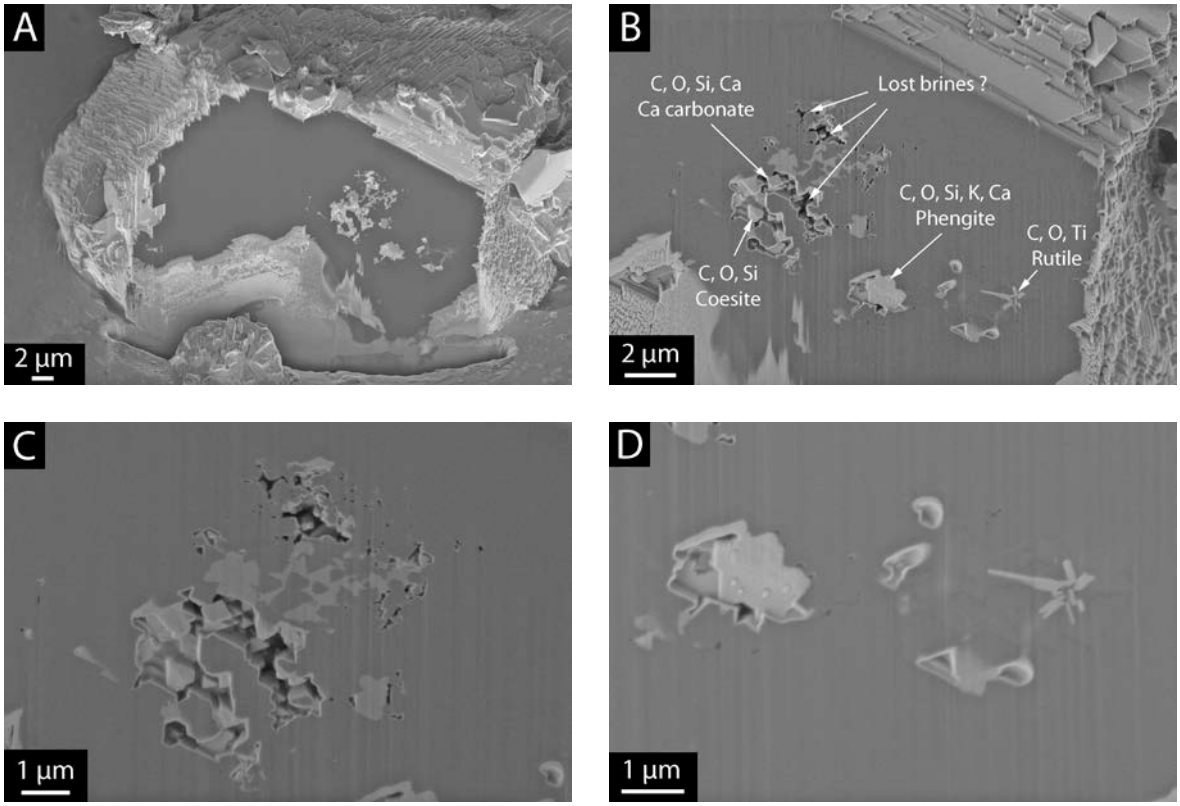

Figure 5

891
892
893

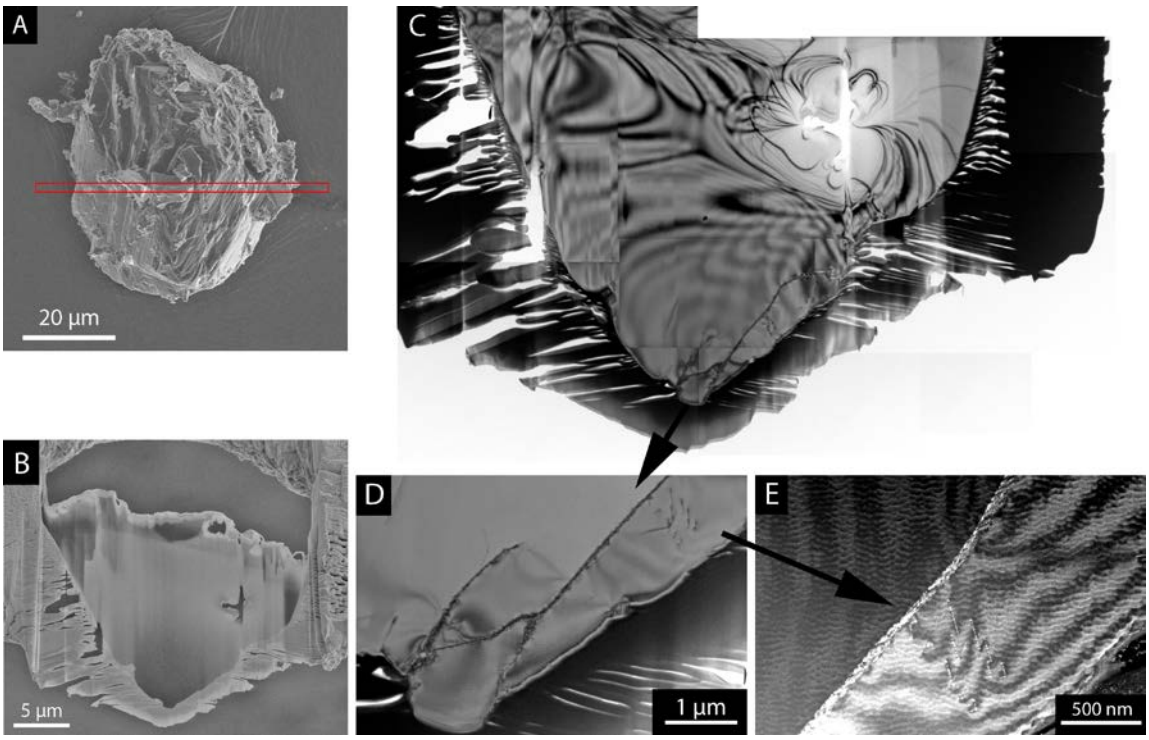

Figure 6

894
895

Table 1: Starting materials

Name	Description	Composition
MELD	Mixture of oxides and carbonates(1)	SiO_2 40.47; Al_2O_3 4.36; MgO 21.07; CaO 9.29; Na_2O 2.36; K_2O 17.57; TiO_2 4.89, about 15 wt.% of CO_2
SIDB	Natural siderite(2)	$(Fe,Mg)CO_3$ In at.%: MgO 2.47; FeO 49.11; MnO 7.17; CaO 0.83
SED(3)	Natural pelagic sediment(4) MD85682 Indian ridge	DRX analysis: 97 % $CaCO_3$ + 3% SiO_2
MORB(3)	Natural mid ocean ridge basalt(5) Indian ridge	DRX analysis: 38.26% $CaAl_2Si_2O_8$ 13.25 % $(Mg_{1.41}Fe_{0.59})$ SiO_4 44.72 % $(Ca_{0.8}Mg_{1.2})Si_2O_6$

(1) After Bureau et al., 2012
(2) After Boulard et al., 2011
(3) DRX analysis after E. Foy
(4) From the *Muséum National d'Histoire Naturelle*'s collection.
(5) Courtesy of Damien Jaujard

Table 2: Summary of experimental conditions and run products

Name	Starting Materials	P GPa	T °C	Duration Hrs	Results and remarks
#H3908 *Set1*	MELD, H_2O-NaCl 10 g/l, G seedsA	7	1400	6:00	D growth on seeds Matrix: D + phengite + $(Ca,Mg)CO_3$ Coesite + rutile Glass + graphite
#H3911 *Set1*	MELD, H_2O-NaCl 30 g/l, G seedsA	7	1400	6:00	D growth on seeds Matrix: D + phengite + $(Ca,Mg)CO_3$ Coesite + rutile Glass + graphite
#H3912 *Set1*	MELD, H_2O-NaCl 30 g/l, G seedsA	7	1300	30:00	D growth on seeds Matrix: D + phengite + $(Ca,Mg)CO_3$ Coesite + rutile + KCl Glass + graphite
#S5970 *Set2*	MELD+SIDB H_2O-NaCl 30 g/l, G seedsB	7	1300	30:00	D growth on seeds Matrix: D + olivine + $(Ca,Mg)CO_3$ KCl Glass + graphite
#H3913 *Set2*	MELD+SIDB H_2O-NaCl 30 g/l, G seedsB	7	1400	6:00	D growth on seeds Matrix: D + olivine+ $(Ca,Mg)CO_3$ Glass + graphite
#H3915 *Set3*	MELD+SIDB H_2O, G seedsB	7	1400	6:00 +	D growth on seeds Matrix: D + olivine + spinel Glass + graphite
#209 *Set4*	MORB+SED H_2O-NaCl 10 g/l, seedsB	7	1300	6:00	D growth not observed Matrix: D + MgO-rich glass Glass + graphite + $(Ca,Fe,Mg)CO_3$
#210 *Set4*	MORB+SED H_2O-NaCl 10 g/l, G seedsB	7	1350	6:00	Slight D growth on seeds Matrix: D + MgO-rich glass Glass + graphite + $(Ca,Fe,Mg)CO_3$
#211 *Set4*	MORB+SED H_2O-NaCl 10 g/l, G seedsB	6	1400	10:00	Fluid lost No real evidence of D growth on seeds Matrix: MgO-rich glass + $CaCO_3$ Glass + graphite

D diamond, G graphite, seedsA: diamonds 40-60 µm, seedsB diamonds 20-30 µm
Runs #209, #210, #211, AuPd capsules; others Pt capsules

Table 3: Typical semi-quantitative EDX analysis of the solid phases (matrix) present in the quenched products from samples from the Set1. Analysis were performed for phases large enough (>1µm). Almost all analysis exhibit a strong contamination, measured as CO_2, due to the powders being deposited on carbon tape, and also due to the presence of diamond seeds. Uncertainties are of about 1 wt.%.

	H3908 pheng	H3908 pheng	H3908 pheng	H3908 pheng	H3911 pheng	H3911 pheng	H3912 pheng	H3912 pheng	H3908 rutile	H3908 carb	H3908 carb	H3911 carb
SiO_2	48,4	49,3	52,9	49,2	51,8	50,1	48,6	50,4	8,4	0,0	1,6	1,0
Al_2O_3	5,8	6,0	5,9	6,1	5,9	6,5	4,8	5,8	2,5	0,0	0,5	0,0
Na_2O	0,0	0,0	0,0	0,0	0,0	0,0	0,0	0,0	0,0	0,0	0,7	0,0
MgO	25,5	24,8	22,9	24,5	23,2	24,6	20,8	23,0	2,6	9,0	11,1	0,6
K_2O	18,4	19,9	18,4	19,5	18,2	18,8	24,5	19,6	5,3	0,0	1,1	0,0
CaO	0,0	0,0	0,0	0,0	0,0	0,0	0,0	0,0	2,4	30,3	39,3	55,0
TiO_2	1,9	0,0	0,0	0,8	0,9	0,0	1,3	1,1	78,9	0,0	0,0	0,0
FeO	0,0	0,0	0,0	0,0	0,0	0,0	0,0	0,0	0,0	0,0	0,0	0,0
CO_2	0,0	0,0	0,0	0,0	0,0	0,0	0,0	0,0	0,0	60,7	45,7	43,4
Total	100,0	100,0	100,0	100,0	100,0	100,0	100,0	100,0	100,0	100,0	100,0	100,0

pheng phengite, carb carbonate

Table 3 : continued, samples from Set2

	S5970 Olivine	S5970 Olivine	S5970 carb	S5970 glass	S5970 glass	H3913 glass	H3913 glass
SiO_2	41,5	47,0	0,0	0,2	0,0	8,4	77,8
Al_2O_3	0,0	0,0	0,0	0,0	0,0	1,7	4,8
Na_2O	0,0	0,0	0,0	0,0	0,0	0,0	0,0
MgO	58,5	53,0	6,3	46,4	100,0	40,3	6,2
K_2O	0,0	0,0	0,0	2,4	0,0	3,8	9,2
CaO	0,0	0,0	0,0	1,7	0,0	36,8	0,9
TiO_2	0,0	0,0	0,0	0,0	0,0	5,3	1,1
FeO	0,0	0,0	0,0	0,0	0,0	0,0	0,0
MnO	0,0	0,0	0,0	0,0	0,0	3,7	0,0
CO_2	0,0	0,0	93,7	49,2	0,0	0,0	0,0
Total	100,0	100,0	100,0	100,0	100,0	100,0	100,0

923 **Table 3 :** continued samples from Set 3 and 4

Set3	H3915 Olivine	H3915 Olivine	H3915 glass	H3915 spinel	Set4	211 carb	209 glass	210 glass	210 glass	210 glass
						0,0	58,7	33,1	41,3	56,3
SiO_2	42,6	41,5	8,9	0,0		0,0	8,4	9,1	23,5	16,7
Al_2O_3	0,0	0,0	0,3	70,2		0,0	1,6	3,6	1,0	5,9
Na_2O	0,0	0,0	0,4	0,0		5,2	3,3	4,1	12,8	7,5
MgO	57,4	58,5	11,6	29,8		0,0	0,0	0,0	0,0	0,0
K_2O	0,0	0,0	4,6	0,0		32,1	24,0	8,3	17,9	12,5
CaO	0,0	0,0	0,9	0,0		0,0	1,3	0,9	0,0	0,0
TiO_2	0,0	0,0	0,0	0,0		1,8	1,8	0,6	3,5	1,0
FeO	0,0	0,0	0,0	0,0		0,0	0,0	0,0	0,0	0,0
MnO	0,0	0,0	0,0	0,0		60,9	0,0	40,3	0,0	0,0
CO_2	0,0	0,0	73,3	0,0		0,0	0,8		0,0	0,0
Total	100,0	100,0	100,0	100,0		100,0	100,0	100,0	100,0	100,0

924

925

926

927

928 **Table 4:** Minerals trapped as inclusions in diamonds, and reference natural basaltic glass
929 M86 (Bureau et al., 1998). Analysis have been performed on thick sections prepared with
930 FIB. The analyses are strongly contaminated in carbon from the diamond-hosts, due to the
931 small size of the inclusions. Uncertainties are of about 1 wt.%.

932

Sample	#H3908 pheng	#H3908 carb	#H3908 rutile	#S5970 Olivine ts	#S5970 carb	M86 glass measured	M86 glass expected
SiO_2	3,0	1,7	0,9	52,9	0,0	47.38	48.65
Al_2O_3	0,0	0,0	0,0	0,5	0,0	14.73	13.93
Na_2O	0,0	0,0	0,0	0,0	0,0	3.51	1.70
MgO	0,0	0,0	0,0	46,6	7,3	8.29	7.48
K_2O	0,3	0,0	0,0	0,0	0,0	0.66	0.62
CaO	0,8	8,6	0,0	0,0	6,6	11.44	11.5
TiO_2	0,0	0,0	18,4	0,0	0,0	2.9	2.83
FeO	0,0	0,0	0,0	0,0	0,0	10.96	10.71
CO_2	96,0	89,7	80,6	0,0	86,0	0,0	0,0
Total	100,0	100,0	100,0	100,0	100,0	100,0	100,0

933

934 pheng phengite, carb carbonate, ts analysis performed on a thin section for TEM

935

936